

Thermoelectrical properties of A-site substituted $\text{Ca}_{1-x}\text{Re}_x\text{MnO}_3$ system

D. Flahaut

National Institute of Advanced Industrial Science and Technology (AIST), 1-8-31 Midorigaoka, Ikeda, Osaka 563-8577, Japan

T. Mihara and R. Funahashi^{a)}

National Institute of Advanced Industrial Science and Technology (AIST), 1-8-31 Midorigaoka, Ikeda, Osaka 563-8577, Japan and CREST-Japan Science and Technology Agency, Ikeda, Osaka 563-8577, Japan

N. Nabeshima

Osaka Electro-Communication University, 18-8 Hatsucho, Neyagawa-shi, Osaka 572-8530, Japan

K. Lee

CREST-Japan Science and Technology Agency, 4-1-8 Honcho, Kawaguchi 332-0012, Japan

H. Ohta and K. Koumoto

CREST-Japan Science and Technology Agency, 4-1-8 Honcho, Kawaguchi 332-0012, Japan and Graduate School of Engineering, Nagoya University, Furo-cho, Chikusa-ku, Nagoya 464-8603, Japan

(Received 25 June 2006; accepted 29 July 2006; published online 31 October 2006)

CaMnO_3 is an electron-doped compound which belongs to the perovskite family. Despite its high Seebeck coefficient S value, the figure of merit at high temperature remains low due to its large resistivity ($\rho(\rho_{300\text{K}}=2\ \Omega\ \text{cm})$). To optimize the performance of this material in terms of thermoelectric properties, several substitutions have been attempted on the Ca site to decrease the ρ . Structure and thermoelectric properties of polycrystalline samples $\text{Ca}_{1-x}\text{A}_x\text{MnO}_3$ ($A=\text{Yb, Tb, Nd, and Ho}$) have been investigated. Although ρ strongly depends on the ionic radius $\langle r_A \rangle$ and carrier concentration, we have shown that the thermal conductivity κ is mainly driven by the atomic weight of the A site and decreases with it. Therefore, it seems that the S , ρ , and κ could be controlled separately. For instance, the highest dimensionless ZT (=0.16) has been obtained at 1000 K in the air for $\text{Ca}_{0.9}\text{Yb}_{0.1}\text{MnO}_3$. © 2006 American Institute of Physics. [DOI: 10.1063/1.2362922]

I. INTRODUCTION

Compared with conventional thermoelectric materials,¹⁻³ metal oxides are very suitable, due to their high thermal and chemical stability, for long time use at high temperatures in air for thermoelectric conversion. The discovery of the NaCo_2O_4 compound⁴ with a large thermoelectric power S ($100\ \mu\text{V K}^{-1}$) and low resistivity ρ ($0.2\ \text{m}\Omega\ \text{cm}$) attracts renewed interest in exploring types of metal oxide materials. Recently, Funahashi *et al.*⁵ have built a thermoelectric device with a high output power density. This module is composed of p -type $\text{Ca}_{2.7}\text{Bi}_{0.3}\text{Co}_4\text{O}_9$ and n -type $\text{La}_{0.9}\text{Bi}_{0.1}\text{NiO}_3$ bulks. The maximum output power obtained for this unicouple is 94 mW at 1073 K ($\Delta T=500\ \text{K}$). The actual n -type, nickelate perovskite has been reported to show a lower negative value of S ($-30\ \mu\text{V K}^{-1}$) and a low resistivity ρ ($1\ \text{m}\Omega\ \text{cm}$). To overcome the lack of n -type materials, some studies have investigated the CaMnO_3 perovskite system which has been suggested as a potential n -type thermoelectric material. This perovskite exhibits a high S but a non-negligible ρ , $-350\ \mu\text{V K}^{-1}$ and $2\ \Omega\ \text{cm}$, respectively. Many studies have been done using this system for colossal magnetoresistance properties at low temperature⁶⁻⁹ and have indicated the predominant role of average ionic radius $\langle r_A \rangle$ of the A site. Substitutions for both Mn and Ca sites, separately, have been

attempted in order to decrease the ρ , and the best power factor ($S^2\rho$) reaches $0.3\ \text{mW m}^{-1}\ \text{K}^{-2}$ for $\text{CaMn}_{0.96}\text{Nb}_{0.4}\text{O}_3$ (Ref. 10) and $0.27\ \text{mW m}^{-1}\ \text{K}^{-2}$ for $\text{Ca}_{0.9}\text{Bi}_{0.1}\text{MnO}_3$ at 1000 K.^{11,12} For these compounds, a high S value has been kept (around $-100\ \mu\text{V K}^{-1}$) and the ρ has been decreased by two scale orders.

In order to discover better n -type materials, we systematically investigate in this present work the thermoelectric properties at high temperature of CaMnO_3 substituted by rare earth (Yb, Tb, Nd, and Ho) on the A site.

II. EXPERIMENT

Polycrystalline samples of $\text{Ca}_{0.9}\text{Re}_{0.1}\text{MnO}_3$ ($A=\text{Yb, Tb, Nd, and Ho}$) were synthesized via solid state reaction in air. The compounds starting from stoichiometric mixtures of CaCO_3 , Mn_2O_3 , Yb_2O_3 , Tb_2O_3 , Ho_2O_3 , and Nd_2O_3 were calcinated at 1073 K in air. Then, the powders were heated at 1273 K for 10 h and at 1475 K for 12 h in air with intermediate grinding. Finally, the products were pressed into pellets and sintered in air at 1573 K for 15 h. The pellets were cooled down to room temperature in the furnace. X-ray powder diffraction (XRD) analysis was carried out with a Rigaku diffractometer using $\text{Cu K}\alpha$ radiation. Lattice parameters were obtained from the Rietveld analysis of the x-ray data.¹³

Resistivity measurements were performed by using a dc standard four-probe method in a temperature range of 300–1100 K in air. The thermoelectromotive forces (ΔV)

^{a)}Author to whom correspondence should be addressed; electronic mail: funahashi-r@aist.go.jp

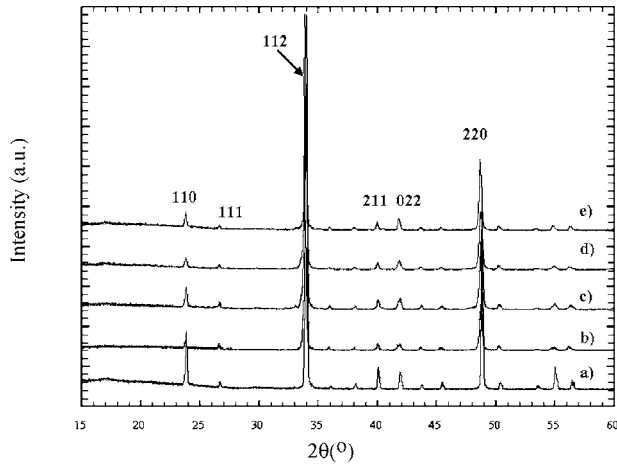


FIG. 1. X-ray patterns of the CaMnO_3 and $\text{Ca}_{0.9}\text{Re}_{0.1}\text{MnO}_3$ samples (Re = Yb, Ho, Tb, and Nd).

and temperature difference (ΔT) were measured at 373–973 K, and S was deduced from the relation $\Delta V/\Delta T$. Two Pt–Pt/Rh thermocouples were attached to both ends of the samples using silver paste. The Pt wires of the thermocouples were used for voltage terminals. Measured S values were reduced by those of Pt wires to obtain the net S values of the samples. Thermal conductivity κ is obtained from the thermal diffusivity, specific heat capacity, and density. Thermal diffusivity and specific heat were measured by a laser flash method (ULVAC-TC3000V) and differential scanning calorimetry (MDSC2910, TA instruments), respectively, in the temperature range of 373–973 K with steps of 100 K.

III. RESULTS AND DISCUSSION

The XRD patterns reported in Fig. 1 indicate that all the samples are single phase with an orthorhombic symmetry. Structure refinements of these samples from x-ray data were performed in the orthorhombic space group $Pnma$ with $a \sim b \sim a_p\sqrt{2}$ and $c \sim 2a_p$. No extra peaks have been observed from rare earth oxide, and no rhombohedral phase has been observed although YbMnO_3 and HoMnO_3 crystallize in a hexagonal perovskite type.¹⁴ Lanthanide size dependence of the cell volume is shown in Fig. 2. The cell volume decreases as the Re^{3+} ionic radius decreases (from Nd^{3+} to Yb^{3+}), which is related to the lanthanide contraction reported also for other rare earth substitutions in the CaMnO_3 perovskite.^{11,15} In that case, substituting the Ca site with a trivalent cation induces Mn(III) cation on the Mn(IV) matrix, whose ionic radius is larger than that of Mn(IV) (0.645 and 0.53 Å, respectively). Nonetheless, this ionic radius change on the Mn site is trivial compared to the cationic size difference between Ca(II) and the smallest rare earth Yb(III) (1.34 and 0.868 Å, respectively). Similarly, the $\langle r_A \rangle$ influences the Mn–O bond distances and Mn–O–Mn angles which are reported in Table I. With the decrease of the $\langle r_A \rangle$, the Mn–O distances increase, whereas Mn–O–Mn angle values decrease. As reported by Kobayashi *et al.* for $(\text{Ca},\text{R}) \times (\text{Mn},\text{Ti})\text{O}_3$ system,¹⁶ the oxygen octahedra around the Mn site become more distorted as the angle value decreases and induce a tilt against each other like zigzag chains. This in-

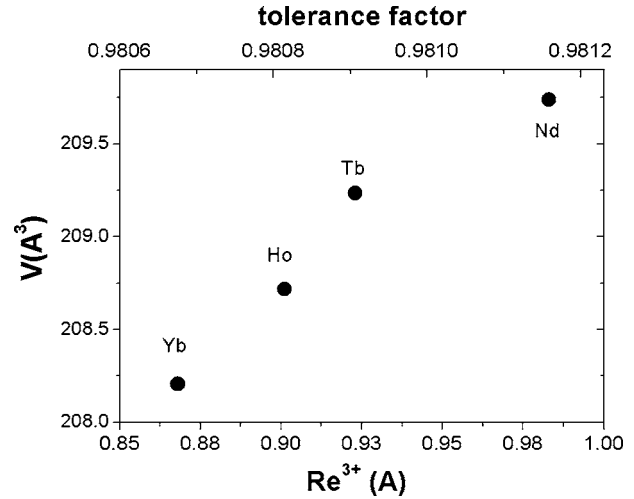


FIG. 2. Lanthanide size and tolerance factor dependence of the cell volume of the CaMnO_3 and $\text{Ca}_{0.9}\text{Re}_{0.1}\text{MnO}_3$ (Re = Yb, Ho, Tb, and Nd).

creases the distortion of an ideal cubic perovskite and can be demonstrated by the evolution of the tolerance factor versus Re^{3+} ionic radius (Fig. 2). This conventional parameter describing the geometric distortion of ABO_3 -type perovskites is defined as $t = (r_A + r_O) / \sqrt{2}(r_B + r_O)$, where r_A , r_B , and r_O are the ionic radii of each atom. Shannon's values of the ionic radius¹⁷ used in the present study for the coordination numbers of A and B atoms are 12 and 6, respectively. Ordinarily, the value of t is within 0.75–1.1 for the perovskites. The cubic structure has a value near 1. As the value of t shifts from 1, geometric distortion becomes gradually larger. As the $\langle r_A \rangle$ decreases, the tolerance factor t becomes smaller, which confirms the enhancement of the orthorhombic distortion.

A. Transport properties

The temperature dependence of the ρ of the samples is shown in Fig. 3. The undoped CaMnO_3 is a n -type semiconductor which exhibits a ρ value around 0.3 Ω cm at room temperature. Substituting the Ca site with rare earth causes a strong decrease of the ρ values of two orders of magnitude, according to the creation of charge carrier content Mn^{3+} in the Mn^{4+} matrix. Moreover, the conduction mode changes from an insulating to a metallic behavior. We must also note that, besides the role of the $\text{Mn}^{4+}/\text{Mn}^{3+}$ ratio, the ρ decreases as the $\langle r_A \rangle$ ionic radius decreases, too, from 10 to 3 $\text{m}\Omega$ cm at 300 K from Nd (0.983 Å) to Yb (0.868 Å), respectively. Many studies report the influence on the transport properties of the $\langle r_A \rangle$ in hole-doped AMnO_3 . Actually, the overlapping of Mn and O orbitals is strongly affected by the $\langle r_A \rangle$, which

TABLE I. Mn–O bond distances and Mn–O–Mn angles of the CaMnO_3 and $\text{Ca}_{0.9}\text{Re}_{0.1}\text{MnO}_3$ compounds (Re = Yb, Ho, Tb, and Nd).

Re	Mn–O (pm)	(Mn–O–Mn) (°)
Yb	191.35	155.0
Ho	191.15	155.9
Tb	191.12	156.6
Nd	190.8	157.8
CaMnO_3	189.9	158

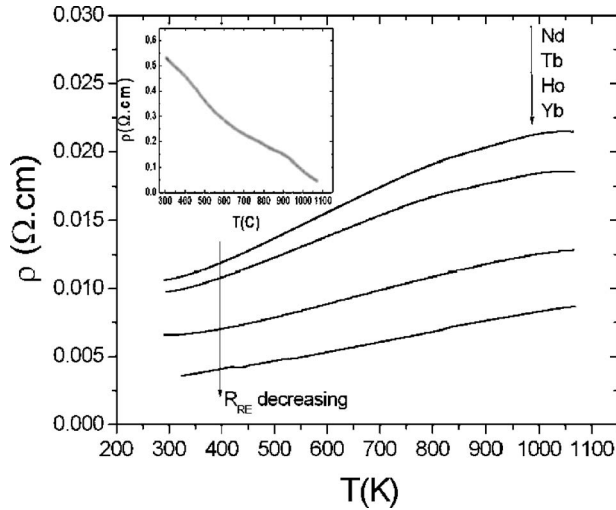


FIG. 3. Temperature (T) dependence of the resistivity (ρ) of the $\text{Ca}_{0.9}\text{Re}_{0.1}\text{MnO}_3$ samples. Inset: resistivity vs temperature of CaMnO_3 .

determines the Mn–O–Mn bond angles. As the conduction is governed by electrons, the decrease of $\langle r_A \rangle$ reduces ρ due to the strength of the bending of the Mn–O–Mn bond, narrowing the e_g electrons conduction bandwidth. Thus, contrary to the hole-doped compounds, the resistivity decreases as $\langle r_A \rangle$ and Mn–O–Mn bond angles decrease for n -type materials.⁸ No substituted CaMnO_3 systems possessing lower ρ than $\text{Ca}_{0.9}\text{Yb}_{0.1}\text{MnO}_3$, 4 m Ω cm at 300 K, have been reported.^{10–12}

B. Thermoelectric properties

Figure 4 shows the S versus temperature for the CaMnO_3 and A -site doped compounds. The negative S value confirms that the dominant electrical carriers are electrons for all the samples. The undoped compound CaMnO_3 shows a large absolute value of S which decreases as the temperature rises. This is related to its low carrier concentration and semiconductor behavior. The rare earth substitution induces a clear decrease of the S value, which is in agreement with the decrease of the ρ and the increase of the charge carrier con-

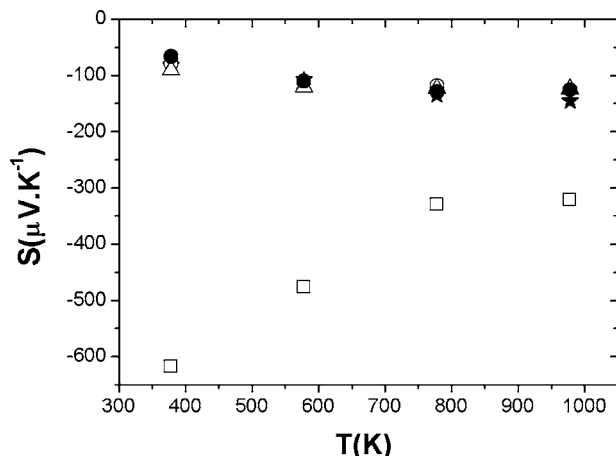


FIG. 4. Temperature T dependence of S of CaMnO_3 (open squares) and $\text{Ca}_{0.9}\text{Re}_{0.1}\text{MnO}_3$ samples [Re=Yb (stars), Ho (closed circles), Tb (open circles), and Nd (triangles)].

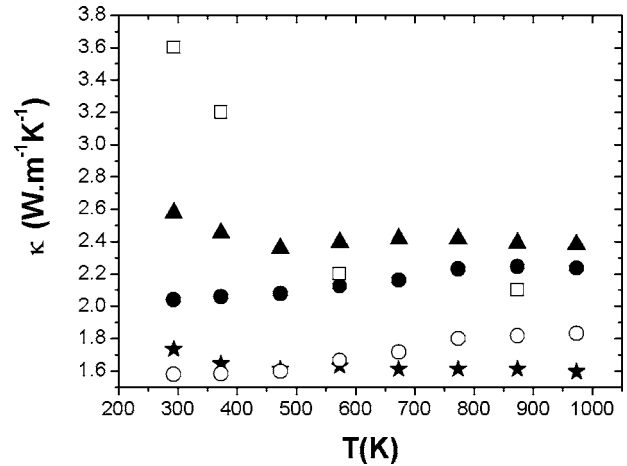


FIG. 5. Temperature T dependence of the thermal conductivity (κ) of CaMnO_3 (open squares) and $\text{Ca}_{0.9}\text{Re}_{0.1}\text{MnO}_3$ samples [Re=Yb (stars), Ho (closed circles), Tb (open circles), and Nd (triangles)].

centration of Mn^{3+} . As S only depends on the concentration and nature of the charge carrier, it is obvious that the S reaches the same value, around $-100 \mu\text{V K}^{-1}$, for all the substituted compounds, accordingly, with the same ratio of $\text{Mn}^{3+}/\text{Mn}^{4+}$. For the substituted compounds, absolute values of S increase linearly with the temperature, from $-80 \mu\text{V K}^{-1}$ at 300 K to $-150 \mu\text{V K}^{-1}$ at 900 K, as previously reported by Ohtaki *et al.*¹¹ in the case of Y^{3+} and Sm^{3+} substitutions. While rare earth size can influence the electronic conductivity, this observation cannot be done for the S measurements.¹⁸

Figure 5 demonstrates the temperature dependence of the thermal conductivity of the samples. κ was calculated from the following formula $\kappa = DC_p d$, where D , C_p , and d are the thermal diffusivity, specific heat capacity, and density, respectively. For comparison, the data for the undoped CaMnO_3 from the work of Ohtaki *et al.*¹¹ is also plotted in this figure. The thermal conductivity values of the substituted compounds are less than those of CaMnO_3 because of their higher electrical conductivity. κ can be expressed by the formula $\kappa = \kappa_l + \kappa_e$, where κ_l is the lattice component and κ_e is the electronic one. For materials with $\rho > 1 \Omega \text{ cm}$, κ_e is negligible. But in our case, the resistivity is very low, a fact which led us to determine the κ_e values by using the Wiedemann-Franz law $\kappa_e = LT\sigma$ ($L = 2.45 \times 10^{-8} \text{ W } \Omega \text{ K}^{-2}$). We found $0.11 \text{ W m}^{-1} \text{ K}^{-1}$ for Nd and $0.29 \text{ W m}^{-1} \text{ K}^{-1}$ for Yb at 1000 K. For all samples, the phonon contribution is more important than the electronic one, whereas κ_e increases as the Re ionic radius decreases. Therefore, κ is mainly assigned to the lattice contribution. As reported by Cong *et al.*,¹⁹ the rare earth substitutions induce the fall of κ_l due to the phonon-lattice defect interaction. Moreover, for the same Re³⁺ content, κ values decrease from Nd to Yb substitution. First, one can suggest that the mass difference between Re and Ca atoms increases the lattice anharmonicity and thus the phonon-phonon interaction. On the other hand, the decrease of the bond angles, which conducts the octahedral distortion, also plays a role in the κ values. Thus, in those compounds, the thermal conductivity strongly depends on the atomic weight, on the A -site weight, and, to a lesser

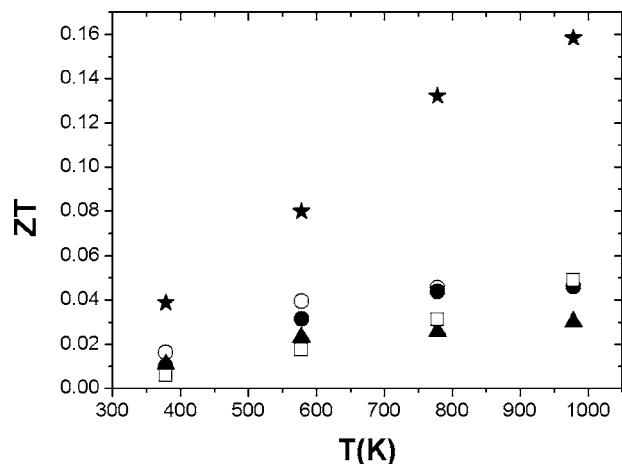


FIG. 6. Temperature T dependence of CaMnO_3 (open squares) and $\text{Ca}_{0.9}\text{Re}_{0.1}\text{MnO}_3$ samples [Re=Yb (stars), Ho (closed circles), Tb (open circles), and Nd (triangles)].

extent, on $\langle r_A \rangle$. So, doping with a heavy and small Re^{3+} minimizes the phonon component of the thermal conductivity. By this, a higher figure of merit could be obtained in these perovskite oxides.

From κ , ρ , and S values, we have calculated the dimensionless figure of merit $ZT = S^2 T / \rho \kappa$. To expect thermoelectric applications, a ZT value around unity has to be reached. Temperature dependence of ZT for $\text{Ca}_{0.9}\text{Re}_{0.1}\text{MnO}_3$ (Re=Yb, Ho, Tb, and Nd) samples is shown in Fig. 6. For all samples, ZT increases with temperature over the whole temperature range. By the fact that S values are independent of the nature of the rare earth and that ρ and κ decrease from Nd to Yb substitution, we expected to obtain higher ZT values than those reported in previous papers.^{12,16} The highest ZT was reached for the Yb substituted sample, $\text{Ca}_{0.9}\text{Yb}_{0.1}\text{MnO}_3$. We obtained a value of 0.16 at 1000 K in air for 10% of Yb on the A site of perovskite, compared to 0.08 for $\text{Ca}_{0.9}\text{Bi}_{0.1}\text{MnO}_3$ (Ref. 11) and 0.06 for $\text{Ca}_{0.9}\text{Pr}_{0.1}\text{MnO}_{2.97}$.¹⁹

IV. CONCLUSION

The high-temperature thermoelectric properties (ρ , S , and κ) of A-site substituted compounds were investigated. By this method, the highest ZT is obtained for the Yb substituted compound and reaches a value of 0.16 at 1000 K in

air. These properties are governed by different parameters. S is only driven by the carrier concentration and nature, although ρ is also linked to the $\langle r_A \rangle$ ionic radius. On the other hand, we have also shown that the atomic weight mainly influences the thermal conductivity values. Accordingly, it seems that we can control all of these three factors individually. This can guide us towards a better thermoelectric material. In a future paper, we will discuss solid solution $\text{Ca}_{1-x}\text{Yb}_x\text{MnO}_3$ and the influence of the Yb content on electrical and thermoelectrical properties.

ACKNOWLEDGMENT

One of the authors (D.F.) acknowledges the Japan Society for the Promotion of Science for awarding her the Foreigner Postdoctoral Fellowship (ID P05864).

- ¹J. F. Nakahara, T. Takeshita, M. J. Tschetter, B. J. Beaudry, and K. A. Gshneider, Jr., *J. Appl. Phys.* **63**, 2331 (1998).
- ²A. Boyer and E. Cisse, *Mater. Sci. Eng., B* **113**, 103 (1992).
- ³G. A. Slack and M. A. Hussain, *J. Appl. Phys.* **70**, 2694 (1991).
- ⁴I. Terasaki, Y. Sasago, and K. Uchinokura, *Phys. Rev. B* **56**, R12685 (1997).
- ⁵R. Funahashi, S. Urata, K. Mizuno, T. Kouuchi, and M. Mikami, *Appl. Phys. Lett.* **85**, 1036 (2004); R. Funahashi, M. Mikami, T. Mihara, S. Urata, and N. Ando, *J. Appl. Phys.* **99**, 066117 (2006).
- ⁶A. Maignan, C. Martin, F. Damay, and B. Raveau, *Chem. Mater.* **10**, 950 (1998).
- ⁷C. Martin, A. Maignan, F. Damay, M. Hervieu, and B. Raveau, *J. Solid State Chem.* **134**, 198 (1997).
- ⁸L. Sudheendra, A. R. Raju, and C. N. Rao, *J. Phys.: Condens. Matter* **15**, 895 (2003).
- ⁹J. Hejmanek, Z. Jirak, M. Marysko, C. Martin, A. Maignan, M. Hervieu, and B. Raveau, *Phys. Rev. B* **60**, 14057 (1999).
- ¹⁰G. Xu, R. Funahashi, I. Matsubara, M. Shikano, and Y. Zhou, *J. Mater. Res.* **17**, 1092 (2002).
- ¹¹M. Ohtaki, H. Koga, T. Tokunaga, K. Eguchi, and H. Arai, *J. Solid State Chem.* **120**, 105 (1995).
- ¹²T. Kobayashi, H. Takizawa, T. Endo, T. Sato, H. Taguchi, and M. Nagao, *J. Solid State Chem.* **92**, 116 (1991).
- ¹³J. Rodriguez-Carvajal, *Physica B* **195**, 55 (1993).
- ¹⁴W. C. Kohler, H. L. Yakel, E. O. Wollan, and J. W. Cable, *Phys. Lett.* **9**, 93 (1964).
- ¹⁵K. Yoshii, H. Abe, and N. Ikeda, *J. Solid State Chem.* **178**, 3615 (2005).
- ¹⁶M. Kobayashi, R. Katsuraya, S. Kurita, M. Yamaguchi, H. Satoh, and N. Kamegashira, *J. Alloys Compd.* **408**, 1173 (2006).
- ¹⁷R. D. Shannon, *Acta Crystallogr., Sect. A: Cryst. Phys., Diffraction, Theor. Gen. Crystallogr.* **32**, 751 (1976).
- ¹⁸I. Medvedeva, A. Maignan, C. Martin, K. Barner, B. Raveau, Yu. Bersenev, N. Mushnikov, and E. Gerasimov, *Physica B* **365**, 114 (2005).
- ¹⁹B. C. Cong, T. Tsuji, P. X. Thao, P. Q. Thanh, and Y. Yamamura, *Physica B* **352**, 18 (2004).